Complete synchronization and generalized synchronization of one-way coupled time-delay systems

Meng Zhan,[1] Xingang Wang,[1] Xiaofeng Gong,[1] G. W. Wei,[2,3] and C.-H. Lai[4]
[1]*Temasek Laboratories, National University of Singapore, Singapore 119260*
[2]*Department of Mathematics, Michigan State University, East Lansing, Michigan 48824, USA*
[3]*Department of Computational Science, National University of Singapore, Singapore 117543*
[4]*Department of Physics, National University of Singapore, Singapore 117542*
(Received 23 May 2003; published 18 September 2003)

The complete synchronization and generalized synchronization (GS) of one-way coupled time-delay systems are studied. We find that GS can be achieved by a single scalar signal, and its synchronization threshold for different delay times shows the *parameter resonance* effect, i.e., we can obtain stable synchronization at a smaller coupling if the delay time of the driven system is chosen such that it is in resonance with the driving system. Near chaos synchronization, the desynchronization dynamics displays *periodic bursts* with the period equal to the delay time of the driven system. These features can be easily applied to the recovery of time-delay systems.

DOI: 10.1103/PhysRevE.68.036208 PACS number(s): 05.45.Xt, 05.45.Vx

Chaos synchronization has aroused great interests in the study of nonlinear dynamics [1] due to the potential application in engineering, and the understanding of complicated phenomena in nature. Different kinds of synchronization have been found: complete synchronization (CS) [2,3], generalized synchronization (GS) [4], phase synchronization [5], and lag synchronization [6,7]. CS means that the coupled systems remain in step with each other in the course of time. It is obvious that CS is the simplest and strongest form among the diverse synchronization behaviors. Only in coupled systems with identical elements (i.e., each component having the same dynamics and parameter set) can we observe CS. In the study of nonidentical coupled systems, particularly in the drive-response systems [using $X(p,t)$ to drive $Y(p',t)$, p and p' being different parameters], GS is observed under sufficiently strong driving: the response system is a function of the driving system, $Y(t)=\Phi(X(t))$. Clearly $\Phi\equiv 1$ for CS, and CS is only a subset of GS. With GS, $Y(t)$ is totally ''slaved,'' and loses its intrinsic chaoticity in the absence of coupling, or in other words, the exponential sensitivity with initial condition. Therefore, all driven systems with different initial conditions under the same driving can be following the same trajectories under GS if there is no other attractor in the phase space.

It is known that chaos synchronization is extensively exploited in secure communication. The initial motivation is very straightforward: one can use the essential characteristics of chaos (temporal complexity and apparent randomness) and hide the information to be transmitted in a chaotic signal, and retrieve it by using the technique of chaos synchronization at the receiver end. Nevertheless, many researchers have found that secure communication based on low-dimensional system is not as secure as we commonly believe, since the low-dimensional chaotic system can be reconstructed easily by the embedding method, and can then be separated from the secure information [8]. Because of this, researchers started to look into chaos synchronization in high-dimensional systems, and have found coupled map lattices (CML) [9] and coupled time-delay systems [10] to be reasonable candidates. Very recently Ref. [11] has proposed a new method based on the CML with supposedly high security. Analytical studies and numerical simulation of CS of coupled time-delay systems have also been extensively investigated [12–14]. In this paper, we mainly study both CS and GS of one-way coupled time-delay systems. In particular, we focus on the relationship between these two modes of synchronization, the critical coupling strengths for synchronization at different delay times, and the desynchronization dynamics.

To be specific, we consider the case of one-way coupled time-delay systems:

$$\dot{x}=f(x,x_{\tau 1}),$$

$$\dot{y}=f(y,y_{\tau 2})+\varepsilon(x-y), \tag{1}$$

where $\dot{x}=f(x,x_\tau)=ax_\tau/(1+x_\tau^b)-cx$ is the Mackey-Glass (MG) equation [10], $a=2$, $b=10$, and $c=1$, $x_\tau=x(t-\tau)$ denotes the time-delayed variable, and ε is the ''coupling constant.'' In this case, τ_1 can be different from τ_2, and GS in the parameter space of τ_1 and τ_2 is the principal focus of study in this paper.

We would like to first highlight some of the properties of a single MG system at the above parameters [10,12]. At $\tau<0.471$, there is a stable fixed point attractor; for $0.471<\tau<1.33$, a stable limit cycle attractor emerges; at $\tau=1.33$, the system starts on a period doubling bifurcation sequence until the accumulation point at $\tau=1.68$. Beyond that ($\tau>1.68$), we find a chaotic attractor at most parameter values of τ, with the number of positive Lyapunov exponents and the information dimension increasing linearly with τ, whereas the metric entropy remaining roughly constant. In other words, at large enough τ, the system has a high-dimensional chaotic attractor.

As a start, let us study CS when the driving and driven systems have the same delay time, $\tau_1=\tau_2=\tau$ at Eqs. (1). A linear stability analysis is performed with a small deviation $\Delta(t)=y(t)-x(t)$ from the synchronization manifold, whose stability is governed by

$$\dot{\Delta}=[\partial_1 f(x,x_\tau)-\varepsilon]\Delta+\partial_2 f(x,x_\tau)\Delta_\tau, \tag{2}$$

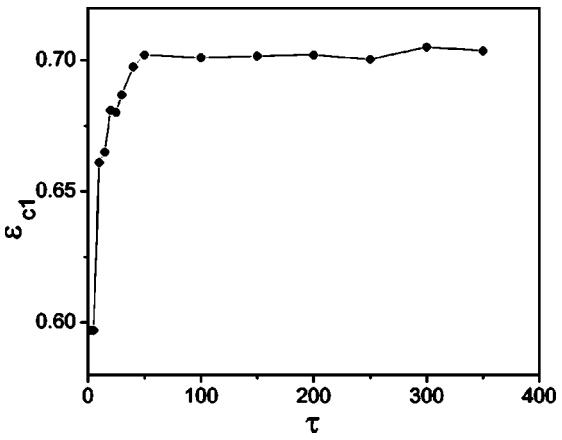

FIG. 1. The dependence of the synchronization threshold for CS, ε_{c1}, on the delay time τ. Above this curve, stable CS can be achieved.

where ∂_1 and ∂_2 are the partial differentials of $f(x,x_\tau)$ with respect to the first and second variables, respectively, and $\Delta_\tau=\Delta(t-\tau)$. As in the treatment of systems described by ordinary differential equations, we can define the largest conditional Lyapunov exponent of CS as [12]

$$\lambda_1(\varepsilon)=\lim_{t\to\infty}\frac{1}{t}\ln\frac{\left\{\int_{-\tau}^{0}\Delta^2(t+\varphi)d\varphi\right\}^{1/2}}{\left\{\int_{-\tau}^{0}\Delta^2(\varphi)d\varphi\right\}^{1/2}}. \tag{3}$$

Clearly $\lambda_1(\varepsilon)$ controls the stability of the complete synchronous state $y(t)=x(t)$. In particular, if $\lambda_1(\varepsilon)<0$, we will be able to observe stable CS.

In Ref. [12], Pyragas has studied CS in Eqs. (1) and found that with increasing τ, the synchronization threshold in the coupling parameter first increases and then saturates to a finite value of ≈ 0.70 (see Fig. 1). (For all the numerical computations in this paper, the fourth-order Runge-Kutta algorithm with a fixed step size of $h=0.01$ is used, and the main numerical results have also been verified by the program DDE23 in MATLAB [15].) As a result, even by transmitting a single scalar variable [x in Eqs. (1)], CS is possible for these systems which, when uncoupled, possess an arbitrarily large number of positive Lyapunov exponents. This is obviously contrary to the intuitive idea that a large number of transmitted signals would be required to suppress the unstable directions of the synchronous state with many positive Lyapunov exponents.

We then ask ourselves the question of what happens if τ_1 is not equal to τ_2. In this case, we know that CS cannot be achieved, but then is stable GS possible? If it is, we would then want to know the relationship between the synchronization threshold for different τ_1 and τ_2. Experimentally, we usually use the auxiliary system method to detect GS: that is, given another identical driven auxiliary system $Z(t)$, GS between $X(t)$ and $Y(t)$ is established with the achievement of CS between $Y(t)$ and $Z(t)$. The coupled systems can be expressed as

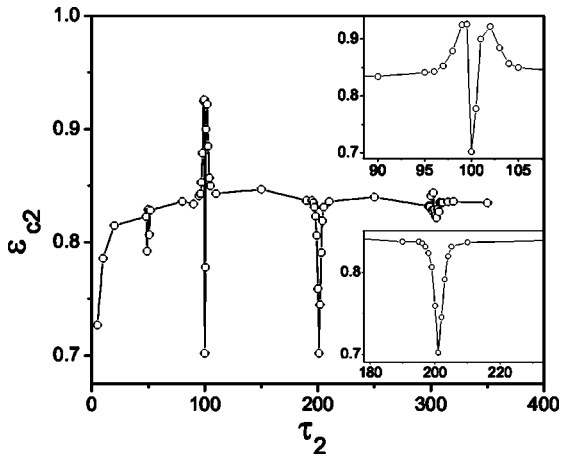

FIG. 2. The dependence of the synchronization threshold for GS, ε_{c2}, on the delay time τ_2. (The delay time of the driving system is fixed at $\tau_1=100$.) The two insets are the blowup of the two regions near $\tau_2=\tau_1=100$ and $\tau_2=2\tau_1=200$.

$$\dot{x}=f(x,x_{\tau 1}),$$

$$\dot{y}=f(y,y_{\tau 2})+\varepsilon(x-y),$$

$$\dot{z}=f(z,z_{\tau 2})+\varepsilon(x-z). \tag{4}$$

In fact, the auxiliary system method detects the local stability of the generalized synchronous state of $Y(t)=\Phi(X(t))$. With $\Lambda(t)=z(t)-y(t)$, we then obtain the linearization stability equation of GS,

$$\dot{\Lambda}=[\partial_1 f(y,y_{\tau 2})-\varepsilon]\Lambda+\partial_2 f(y,y_{\tau 2})\Lambda_\tau. \tag{5}$$

Similarly, we define the largest conditional Lyapunov exponent as

$$\lambda_2(\varepsilon)=\lim_{t\to\infty}\frac{1}{t}\ln\frac{\left\{\int_{-\tau 2}^{0}\Lambda^2(t+\varphi)d\varphi\right\}^{1/2}}{\left\{\int_{-\tau 2}^{0}\Lambda^2(\varphi)d\varphi\right\}^{1/2}}. \tag{6}$$

Figure 2 shows the relation between ε_{c2} and τ_2 with a fixed delay time for the driving system, $\tau_1=100$. Similar to CS in Fig. 1, with increasing τ_2, the synchronization threshold ε_{c2} increases and then saturates to a finite value of 0.84 approximately. Thus even GS, just as CS, can be achieved by a single scalar signal. Apart from this similarity, however, we also observe sharp dips located at the (resonance) parameter values: near $\tau_2=100=\tau_1$ and $\tau_2=201\approx 2\tau_1$ (see the two magnified figures in Fig. 2), and those near $\tau_2=49\approx\tau_1/2$ and $\tau_2=305\approx 3\tau_1$ with some apparent fluctuations. This *parameter resonance* effect in GS certainly reveals how the nonlinear dynamics of coupled systems changes with the matching of two delay time scales. Moreover, its universality has been confirmed for different τ_1 in Fig. 3, plotted with the solid points denoting the local minima of the resonance peaks. Nearly all of these minima are located near the resonance values: $\tau_2=\tau_1/2,\tau_1,2\tau_1,3\tau_1$. Note that τ_1 varies over a very

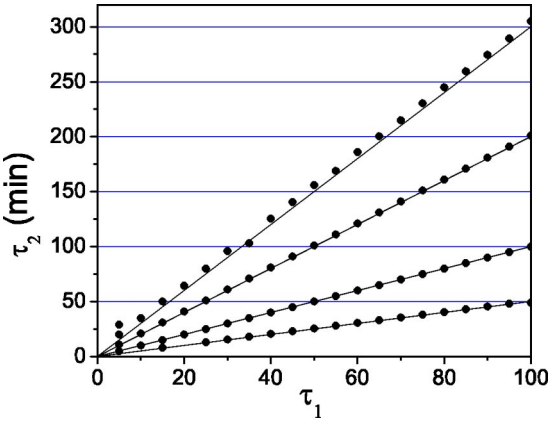

FIG. 3. The universality of the parameter resonance effect. We find nearly all of resonance positions stay at or around $\tau_2=\tau_1/2$, τ_1, $2\tau_1$, and $3\tau_1$.

wide parameter region from 5 to 100. The higher-order resonance peaks (for example, $\tau_2\approx\tau_1/3$ or $\tau_2\approx 4\tau_1$) do not seem to show up well, perhaps because of the coarse scanning we carried out.

To try to understand this resonance phenomenon better, we plot in Fig. 4 λ_1 (solid circles) and λ_2 (hollow circles) vs coupling ε for $\tau_1=\tau_2=\tau=100$. Note that we can discuss the stabilities of both CS and GS only for identical coupled systems. After the transition to CS at $\lambda_1(\varepsilon)$, the manifold of GS with $Y(t)=\Phi(X(t))$ degenerates to that of CS with $Y(t)\equiv X(t)$, so, $\lambda_2(\varepsilon)$ is equal to $\lambda_1(\varepsilon)$ for $\varepsilon>\varepsilon_{c1}$. An important observation from Fig. 4 is that the coupled systems transit to generalized synchronous chaos directly, and the synchronization thresholds of CS and GS are *identical* [16], $\varepsilon_{c1}=\varepsilon_{c2}$. (It should be emphasized that the pattern in Fig. 4 is independent of the chosen value of τ.) This feature closely connects with the parameter resonance effect in Fig. 2, and we can at least understand in an intuitive way the resonance (dip) to the common threshold of value of ≈ 0.70 for GS and CS at $\tau_2\approx 100$.

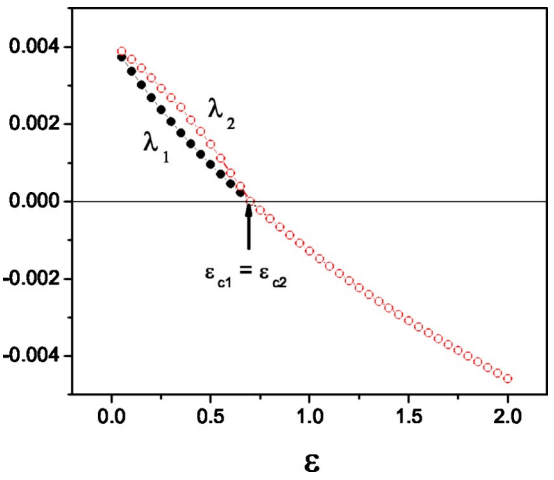

FIG. 4. The largest conditional Lyapunov exponent of CS, λ_1 (solid circles), and that of GS, λ_2 (hollow circles), as a function of the coupling ε for $\tau_1=\tau_2=\tau=100$.

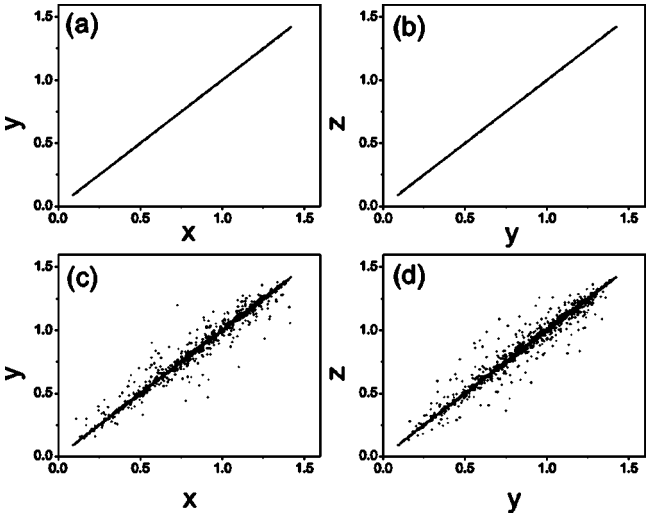

FIG. 5. The dynamics in the vicinity of the synchronization threshold for (a), (b) $\varepsilon=0.71$ (above ε_c) and (c), (d) $\varepsilon=0.69$ (below ε_c). $\tau_1=\tau_2=\tau=100$. $\varepsilon_{c2}=\varepsilon_{c1}=\varepsilon_c\approx 0.702$.

In order to understand the synchronization mechanism, it will be important to follow the dynamics in the vicinity of the synchronization threshold. Figure 5 shows the relation between x, y, and z in Eqs. (4), with $\tau_1=\tau_2=100$, for $\varepsilon=0.71$ [Figs. 5(a,b)] and $\varepsilon=0.69$ [Figs. 5(c,d)], respectively. Above the synchronization threshold, $\varepsilon_{c2}=\varepsilon_{c1}\approx 0.702$, both perfect CS [Fig. 5(a)] and GS [Fig. 5(b)] are observed; below it, CS [Fig. 5(c)] and GS [Fig. 5(d)] lose stability simultaneously, and the desynchronization behavior shows bursts out of the diagonal occasionally with rough synchronization at most time. The time traces of the difference $x-y$ are displayed in Figs. 6(a) and 6(b). In Fig. 6(a), the total observation time is 4×10^5 after discarding the long transient data, with one out of every 20 points plotted. The intermittent behavior is reminiscent of the usual desynchronous chaotic

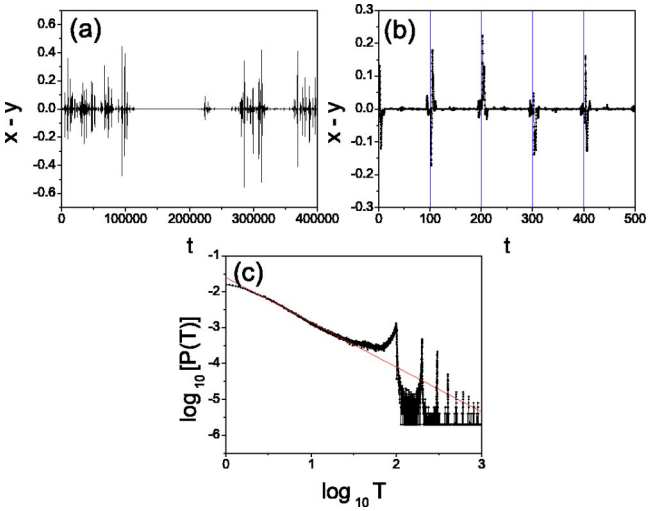

FIG. 6. The desynchronization dynamics of the driving and the response systems for the parameter values $\varepsilon=0.69$. (a) and (b) The time evolution of the difference $x-y$. (c) The distribution of the laminar phase of $x-y$.

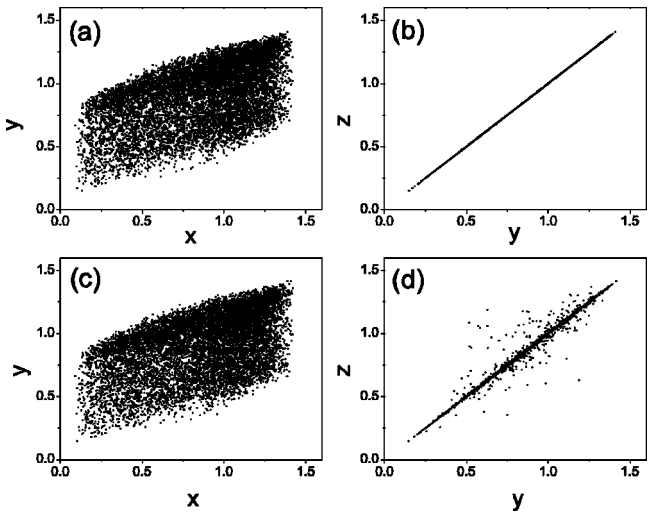

FIG. 7. Same as Fig. 5 but for a nonidentical coupled time-delay system. The parameters are $\tau_1=100$ and $\tau_2=90$, and now $\varepsilon_{c2}\approx 0.834$. (a) and (b)—$\varepsilon=0.85$ (above ε_{c2}). (c) and (d)—$\varepsilon=0.82$ (below ε_{c2}).

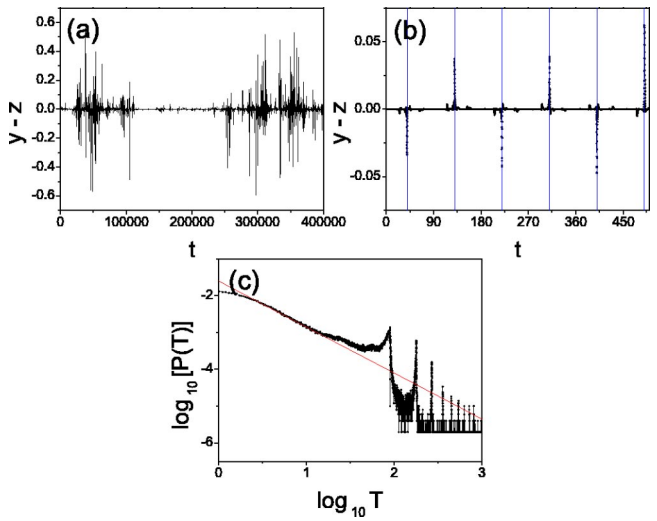

FIG. 8. The desynchronization dynamics near a stable GS state. $\tau_1=100$ and $\tau_2=90$. The interval of the grid lines in (b) is 90.

behavior of on-off intermittency, in which the system dynamics typically stays most of time in the vicinity of the synchronization manifold with occasional bursts out of it. A remarkable finding in this investigation is the more detailed structures [in Fig. 6(b)]: periodic bursts with a period that is equal to the delay time. Now the observed part is the first 500 time units in Fig. 6(a) in 0.1 intervals. Figure 6(c) presents the histogram distribution of laminar phases with the sampling number being 5×10^5 and the critical value d to demarcate the ''off'' state being 0.1. For $T>100$, because of the periodicity of the trajectory, it also displays periodic bursts at $n\tau$, $n=1,2,3,\ldots$. There is strong suggestion of a power-law distribution, $P(T)\propto T^{-\alpha}$, with $\alpha\approx 1.25$. For different d, say $d=0.01$, similar distribution with the same scaling is obtained. The possible reason for α deviating from the normal exponent $\alpha=1.5$ for simple on-off intermittency is probably because the dynamics is high dimensional [13].

The characteristics of the desynchronization dynamics with on-off intermittency and periodic bursts appear to be general. Similar to Fig. 5, but now with $\tau_1=100$ and $\tau_2=90$, the behaviors of y vs x and z vs x are plotted for $\varepsilon=0.85$ [Figs. 7(a) and 7(b)] and $\varepsilon=0.82$ [Figs. 7(c) and 7(d)], respectively. (Recall that $\varepsilon_{c2}\approx 0.834$.) In Figs. 7(a) and 7(b), GS without CS $[y(t)=z(t)\neq x(t)]$ is observed. From Figs. 7(a) and 7(c), we cannot tell the difference between the driving and response systems, while the transition to the identity of two driven systems y and z [from Figs. 7(d) to 7(b)] indicates the establishment of GS. Similar to Fig. 6, on-off intermittency at large time scale [Fig. 8(a)], periodic bursts with the delay time of the driven system $\tau_2=90$ as the period at small time scale [Fig. 8(b)], and the distribution with similar pattern and same scaling [Fig. 8(c)], are again observed. We have verified that these results are not affected by the existence of small noise levels. Three independent noise sources with a strength of 10^{-3} and Gaussian distribution are added to the right-hand side of Eqs. (4). The periodic bursts persist even with the coupling larger than the critical value—hence the environmental noise smooths out the transition and enlarges the parameter region of the phenomenon. This robustness certainly is very useful for experimental application.

Chaos synchronization of coupled time-delay systems is exploited in secure communication for two important reasons: the system is of high dimensionality with multiple positive Lyapunov exponents, and it is easy to construct. On the other hand, a special embedding approach recently proposed in Ref. [17] seems to suggest that communication using chaos synchronization of time-delay systems is not as secure as one might expect. The essential idea of the approach is simple: in the three-dimensional space $(x,x_{\tau 0},\dot{x})$, the dynamics of the time-delay system is projected to a smooth manifold, $\dot{x}-f(x,x_{\tau 0})=0$, in contrast to the high dimensionality of the original phase space. In a similar space $(x,x_{\tau},\dot{x})$, however, with $\tau\neq\tau_0$, the trajectory is no longer restricted to a smooth hypersurface. Through a search in τ space, we can identify the delay time τ_0, reconstruct the chaotic dynamics, and unmask the hidden message.

In fact, the findings in this paper can also be applied easily to recover time-delay systems. Taking advantage of the ''parameter resonance'' effect, we can search the threshold coupling strength for the driving at different τ_1. The position of a drop in ε_{c2} marks the approximate value of τ_2. Another easier approach is based on the desynchronization dynamics in Fig. 8(b). We can use an arbitrary time-delay system to drive two secured systems (which we want to attack) with the same parameter set and different initial conditions. This time we tune the driving strength from above to below the critical value. Below the critical GS, the periodic bursts in the difference in the state variables will uncover the secret of their delay-time parameter. Because ε_{c2} is not sensitive with the changing of τ_1 and τ_2, except in the parameter resonance region, and the coupled systems are not sensitive to the ambient noise, this method should be realizable under experimental conditions.

In conclusion, CS and GS of unidirectionally coupled time-delay systems have been investigated. First, similar to CS, GS can be achieved through only one driving signal, and the threshold coupling strength saturates at a finite value as the time-delay increases, except for the parameter resonance effect, which is induced by the matching of the delay times between the driving and response systems. The second significant observation, which can be applied directly in the breaking of chaos-based secure communication, is that the desynchronization dynamics of both CS and GS is identified with periodic bursts. Since an electronic analog of the MG system has been implemented [18], we believe our numerical results are generic and consequently observable in laboratory experiments.

[1] A.S. Pikovsky, M.G. Rosenblum, and J. Kurths, *Synchronization—A Unified Approach to Nonlinear Science* (Cambridge University Press, Cambridge, England, 2001); L.M. Pecora, T.L. Carroll, G.A. Johnson, D.J. Mar, and J.F. Heagy, Chaos **7**, 520 (1997).

[2] L.M. Pecora and T.L. Carroll, Phys. Rev. Lett. **64**, 821 (1990); **80**, 2109 (1998).

[3] J. Yang, G. Hu, and J. Xiao, Phys. Rev. Lett. **80**, 496 (1998); M. Zhan, G. Hu, and J. Yang, Phys. Rev. E **62**, 2963 (2000); G.W. Wei, M. Zhan, and C.-H. Lai, Phys. Rev. Lett. **89**, 284103 (2002).

[4] N.F. Rulkov, M.M. Sushchik, L.S. Tsimring, and H.D.I. Abarbanel, Phys. Rev. E **51**, 980 (1995); L.M. Pecora, T.L. Carroll, and J.F. Heagy, *ibid.* **52**, 3420 (1995); L. Kocarev and U. Parlitz, Phys. Rev. Lett. **76**, 1816 (1996).

[5] M.G. Rosenblum, A.S. Pikovsky, and J. Kurths, Phys. Rev. Lett. **76**, 1804 (1996); A.S. Pikovsky, M.G. Rosenblum, G.V. Osipov, and J. Kurths, Physica D **104**, 219 (1997); T. Yalcinkaya and Y.C. Lai, Phys. Rev. Lett. **79**, 3885 (1997).

[6] M.G. Rosenblem, A.S. Pikovsky, and J. Kurths, Phys. Rev. Lett. **78**, 4193 (1997).

[7] S. Rim, I. Kim, P. Kang, Y.-J. Park, and C-M. Kim, Phys. Rev. E **66**, 015205 (2002); D. Pazo, M.A. Zaks, and J. Kurths, Chaos **13**, 309 (2003); M. Zhan, G.W. Wei, and C.-H. Lai, Phys. Rev. E **65**, 036202 (2002).

[8] G. Perez and H. Cerdeira, Phys. Rev. Lett. **74**, 1970 (1995); K.M. Short and A.T. Parker, Phys. Rev. E **58**, 1159 (1998).

[9] K. Kaneko, *Theory and Applications of Coupled Map Lattices* (Wiley, New York, 1993).

[10] M.C. Mackey and L. Glass, Science **197**, 287 (1977); J.D. Farmer, Physica D **4**, 366 (1982); P. Grassberger and I. Procaccia, *ibid.* **9**, 189 (1983).

[11] S. Wang, J. Kuang, J. Li, Y. Luo, H. Lu, and G. Hu, Phys. Rev. E **66**, 065202 (2002).

[12] K. Pyragas, Phys. Rev. E **58**, 3067 (1998).

[13] M.J. Bunner and W. Just, Phys. Rev. E **58**, R4072 (1998).

[14] S. Boccaletti, D.L. Valladares, J. Kurths, D. Maza, and H. Mancini, Phys. Rev. E **61**, 3712 (2000).

[15] L.F. Shampine and S. Thompson, Appl. Numer. Math. **37**, 441 (2001).

[16] K. Pyragas, Phys. Rev. E **54**, R4508 (1996); M.S. Vieira and A.J. Lichtenberg, *ibid.* **56**, R3741 (1997).

[17] M.J. Bunner, T. Meyer, A. Kittel, and J. Parisi, Phys. Rev. E **56**, 5083 (1997); R. Hegger, M.J. Bunner, H. Kantz, and A. Giaquinta, Phys. Rev. Lett. **81**, 558 (1998); C. Zhou and C.-H. Lai, Phys. Rev. E **60**, 320 (1999).

[18] A. Namajunas, K. Pyragas, and A. Tamasevicius, Phys. Lett. A **201**, 42 (1995).